

Analysis of lossy multiconductor transmission lines and application of a crosstalk canceling algorithm

Reuven Ianconescu

*Shenkar College of Engineering and Design 12, Anna Frank St., Ramat Gan, Israel**

Vladimir Vulfin

*Department of Electrical and Computer Engineering,
Ben-Gurion University of the Negev, Beer Sheva 84105, Israel[†]*

We showed in a previous work that it is possible to transmit N signals without crosstalk or return loss through a lossless multiconductor transmission line of $N+1$ conductors. Such algorithm can increase the data rate twice (in absence of noise), relative to the usual transmission of differential signals. In the current work we analyze lossy multiconductor transmission lines and test the above algorithm on the lossy lines.

*Electronic address: riancon@gmail.com, riancon@shenkar.ac.il

[†]Electronic address: vlad2042@yahoo.com

I. INTRODUCTION

In a previous work [1], we derived an algorithm for transmitting the maximum possible number of signals without crosstalk or return loss, in lossless multiconductor transmission lines (MTL). Using this algorithm on a MTL of $N + 1$ conductors, one is able to transmit N independent unaltered signals. The algorithm defines pre-processing and post-processing units to be interfaced at the input and output of the lossless MTL, which are able to completely eliminate crosstalk and return loss. In the current work we shall make a profound analysis of lossy MTL, and evaluate the efficiency of the above algorithm for lossy MTL, for which the properties are necessarily frequency dependent. Some preliminary results have been presented in [2].

Knowing that the applications of fast data transmission on MTL (like flat cables, backplanes, etc.) use differential signals between pairs of conductors, the application of such an algorithm has the potential to roughly double the information rate. In addition, the usage of differential signals does not allow a perfect match of the MTL [3–10].

The outline is as follows: In section II, we explain the theoretical background developed in [1] and point on the changes that occur in the lossy case. Some classification of modes according to their immunity to noise is also presented.

In section III we show the results of our simulations for several cases: copper losses only, dielectric losses only and copper and dielectric losses together. From the analysis it results that radiation losses exist too in the MTL configuration that we study. It is also shown how one can extract the parameters of a homogeneous free space configuration, specifically the characteristic impedance matrix from the results of the inhomogeneous analysis.

In section IV we analyze the consistency of the simulation results, i.e. how the results for the different cases are connected to each other. We show in this section that the simulations detected radiation losses in all the above cases.

In section V we show that although modes of MTL do not need to match results of two-conductor MTL, we get a good match between them, in cases this is physically justified. In section VI we apply the crosstalk canceling algorithm developed in [1] to the lossy case and examine its performance. The work is ended by some concluding remarks.

Note: through this work, the unit matrix is noted by \mathbf{U} , to avoid confusion with current vectors \mathbf{I} . All the matrix transpose operations are transpose and no conjugate.

II. THEORETICAL BACKGROUND

The full details of this theoretical background are in [1], and we show here the main results that we need in the current work.

We define the scattering matrix of the MTL for equal port impedances R . The near end ports are numbered $1, 2, \dots, N$ and the far end ports are numbered $N + 1, N + 2, \dots, 2N$. The forward voltages into the ports are $V_1^+, V_2^+, \dots, V_N^+, V_{N+1}^+, V_{N+2}^+, \dots, V_{2N}^+$ and will be grouped as \mathbf{V}_{ne}^+ at the near end (i.e. from 1 to N) and \mathbf{V}_{fe}^+ at the far end (i.e. from $N + 1$ to $2N$). We use the same grouping for the backward voltages: \mathbf{V}_{ne}^- and \mathbf{V}_{fe}^- . The scattering matrix is grouped into four $N \times N$ submatrices, as follows

$$\begin{pmatrix} \mathbf{V}_{ne}^- \\ \mathbf{V}_{fe}^- \end{pmatrix} = \begin{pmatrix} \mathbf{\Gamma} & \boldsymbol{\tau} \\ \boldsymbol{\tau} & \mathbf{\Gamma} \end{pmatrix} \begin{pmatrix} \mathbf{V}_{ne}^+ \\ \mathbf{V}_{fe}^+ \end{pmatrix}, \quad (1)$$

where the submatrices $\mathbf{\Gamma}$ and $\boldsymbol{\tau}$ are symmetric, i.e.

$$\mathbf{\Gamma} = \mathbf{\Gamma}^T \quad (2)$$

and

$$\boldsymbol{\tau} = \boldsymbol{\tau}^T \quad (3)$$

The MTL may equally be described by a generalized ABCD matrix as follows

$$\begin{pmatrix} \mathbf{V}_{ne} \\ \mathbf{I}_{ne} \end{pmatrix} = \begin{pmatrix} \mathbf{A} & \mathbf{B} \\ \mathbf{C} & \mathbf{D} \end{pmatrix} \begin{pmatrix} \mathbf{V}_{fe} \\ -\mathbf{I}_{fe} \end{pmatrix}, \quad (4)$$

where \mathbf{A} , \mathbf{B} , \mathbf{C} and \mathbf{D} are $N \times N$ submatrices, derived from $\mathbf{\Gamma}$ and $\boldsymbol{\tau}$ as follows:

$$\mathbf{A} = \frac{1}{2}[\boldsymbol{\tau} + (\mathbf{U} + \mathbf{\Gamma})\boldsymbol{\tau}^{-1}(\mathbf{U} - \mathbf{\Gamma})], \quad (5)$$

$$\mathbf{B} = \frac{R}{2}[-\boldsymbol{\tau} + (\mathbf{U} + \mathbf{\Gamma})\boldsymbol{\tau}^{-1}(\mathbf{U} + \mathbf{\Gamma})], \quad (6)$$

$$\mathbf{C} = \frac{1}{2R}[-\boldsymbol{\tau} + (\mathbf{U} - \mathbf{\Gamma})\boldsymbol{\tau}^{-1}(\mathbf{U} - \mathbf{\Gamma})], \quad (7)$$

and

$$\mathbf{D} = \frac{1}{2}[\boldsymbol{\tau} + (\mathbf{U} - \mathbf{\Gamma})\boldsymbol{\tau}^{-1}(\mathbf{U} + \mathbf{\Gamma})], \quad (8)$$

Using properties (2) and (3), we remark that

$$\mathbf{A} = \mathbf{D}^T \quad (9)$$

The above relations can be inverted, i.e. if one has the ABCD description, one obtains the scattering matrix description as follows:

$$\boldsymbol{\tau} = 2[\mathbf{A} + \mathbf{B}/R + R\mathbf{C} + \mathbf{D}]^{-1}. \quad (10)$$

and

$$\boldsymbol{\Gamma} = -\frac{1}{2}\boldsymbol{\tau}[\mathbf{A} - \mathbf{B}/R + R\mathbf{C} - \mathbf{D}] \quad (11)$$

The submatrices \mathbf{A} , \mathbf{B} , \mathbf{C} and \mathbf{D} are diagonalized by

$$\mathbf{A}' = \mathbf{T}_I^T \mathbf{A} \mathbf{T}_V, \quad (12)$$

$$\mathbf{B}' = \mathbf{T}_I^T \mathbf{B} \mathbf{T}_I, \quad (13)$$

$$\mathbf{C}' = \mathbf{T}_V^T \mathbf{C} \mathbf{T}_V, \quad (14)$$

and

$$\mathbf{D}' = \mathbf{T}_V^T \mathbf{D} \mathbf{T}_I, \quad (15)$$

where the transformations \mathbf{T}_V and \mathbf{T}_I satisfy the relation

$$\mathbf{T}_V^T \mathbf{T}_I = \mathbf{U}, \quad (16)$$

and one has to diagonalize \mathbf{A} (or \mathbf{D}) to obtain them, and then apply them on the other matrices.

It is to be mentioned that in general the transformations \mathbf{T}_V and \mathbf{T}_I are complex and frequency dependent. The imaginary part is due to losses and the frequency dependence is due to losses and/or due to the frequency dependence of the relative dielectric constant. However, dielectric constant may be *almost* frequency independent, at least in a given frequency range. We used in [1] a frequency independent dielectric constant, and no losses, hence we obtained *real* and *frequency independent* transformations \mathbf{T}_V and \mathbf{T}_I . With losses, the transformations are frequency dependent and have imaginary values, however, for small losses the frequency dependence is weak and the imaginary parts are small.

From the diagonal matrices in Eqs. (12)-(15) one obtains the eigenvalues of the characteristic impedance matrix:

$$Z'_0 = \sqrt{B'/C'}, \quad (17)$$

and the electric delay of the modes θ given by

$$\theta = \arccos(A'), \quad (18)$$

from which one obtains the equivalent relative dielectric constant of the modes ϵ_{eq} , or its square root, the refraction index n

$$n = \sqrt{\epsilon_{eq}} = \frac{c\theta}{2\pi fl}. \quad (19)$$

It is to be mentioned that the values of Z'_0 , θ and ϵ_{eq} are real for lossless MTL, but have imaginary values in the lossy case.

The connection between the characteristic impedance matrix and its eigenvalues matrix \mathbf{Z}'_0 is given by

$$\mathbf{Z}'_0 = \mathbf{T}_I^T \mathbf{Z}_0 \mathbf{T}_I. \quad (20)$$

A. The special case of homogeneous media

In [3] it is shown that for a MTL in homogeneous medium, one can express the voltage-current vector pair at the near end as function of the voltage-current at the far end by the ABCD representation, so that

$$\begin{aligned} \mathbf{A} &= \mathbf{D} = \mathbf{U} \cos(\theta) \\ \mathbf{B} &= j\mathbf{Z}_0 \sin(\theta) \\ \mathbf{C} &= j\mathbf{Y}_0 \sin(\theta) \end{aligned} \quad (21)$$

where $\mathbf{Y}_0 = \mathbf{Z}_0^{-1}$ is the characteristic admittance matrix and

$$\theta = \frac{2\pi fl}{c} \sqrt{\epsilon_r} \quad (22)$$

is the propagation shift angle of the whole voltage-current wave.

In this case \mathbf{A} and \mathbf{D} being diagonal with equal elements, they are diagonalized by any orthogonal matrix, so that one cannot find \mathbf{T}_V or \mathbf{T}_I from them. Instead, one has to diagonalize \mathbf{Z}_0 which is symmetric and from it one obtains the orthogonal matrix $\mathbf{T}_V = \mathbf{T}_I \equiv \mathbf{T}$, so that

$$\mathbf{Z}'_0 = \mathbf{T}^T \mathbf{Z}_0 \mathbf{T}, \quad (23)$$

B. Scheme for a matched and crosstalk free transmission

We summarize in this subsection the scheme for a matched and crosstalk free transmission [1], shown in Figure 1. The line is fed by the maximum number of independent generator

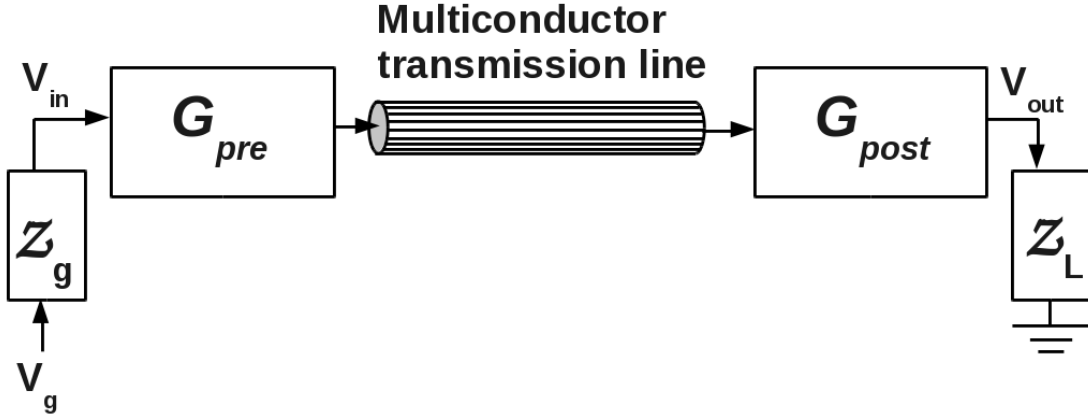


FIG. 1: Multiconductor communication implementing a matched and crosstalk free transmission scheme. A pre-processing transformation unit is implemented at the input of the MTL and a post-processing transformation unit is implemented at the output of the line.

signals \mathbf{V}_{g_i} , for $i = 1, 2..N$, each having the internal impedance Z_{g_i} and loaded at the far end by the loads Z_{L_i} , so that the generator and load impedances are described by diagonal matrices \mathbf{Z}_g and \mathbf{Z}_L . In general, \mathbf{Z}_g and \mathbf{Z}_L may be complex, but matching a complex load to transmission line requires more sophistication even in the one dimensional case, so for the purpose of this work, \mathbf{Z}_g and \mathbf{Z}_L are considered real. The pre and post-processing transformations are computed by

$$\mathbf{G}_{post} = \sqrt{\mathbf{Z}_L \mathbf{Z}'_0^{-1} \mathbf{T}_V^{-1}}. \quad (24)$$

and

$$\mathbf{G}_{pre} = \mathbf{T}_V \sqrt{\mathbf{Z}'_0 \mathbf{Z}_g^{-1}}. \quad (25)$$

We remark that both \mathbf{G}_{pre} and \mathbf{G}_{post} are easily computed because \mathbf{Z}_L , \mathbf{Z}_g and \mathbf{Z}'_0 are diagonal matrices. \mathbf{G}_{pre} and \mathbf{G}_{post} are real in the lossless case, but complex in case of losses (because \mathbf{T}_V is complex). Because we are able to implement real pre and post-processing transformations and those matrices are complex, there is some degradation in the performance of the algorithm due to losses. This issue is further discussed in section VI.

When using the processing units, the relations between \mathbf{V}_{in} , \mathbf{V}_{out} and \mathbf{V}_g are

$$\mathbf{V}_{in} = \frac{1}{2}\mathbf{V}_g, \quad (26)$$

and

$$\mathbf{V}_{out} = \sqrt{\mathbf{Z}_L \mathbf{Z}_g^{-1}} \mathbf{V}_{in} \exp(-j\boldsymbol{\theta}), \quad (27)$$

where $\exp(-j\boldsymbol{\theta})$ is a diagonal matrix describing the delays of the modes, see Eq. (19).

C. Classification of modes by their immunity to noise

We shall discuss in this section the properties of modes in what concerns their immunity to noise, where the noise is any random voltage due to electromagnetic interference for example. To simplify and to be able to use analytic results as examples, we consider here homogeneous medium so that $\mathbf{T}_V = \mathbf{T}_I \equiv \mathbf{T}$ and lossless cases, so that the characteristic impedance matrix is real.

In the context of three conductors, i.e. two conductors and ground we know there are two modes, which we usually call the differential mode and the common mode. It is to be mentioned that this strict classification is valid if the geometry of *both* conductors relative to the ground is identical, as for the examples in Figure 2. Such configurations have a



FIG. 2: Cross sections examples of two conductors having the same geometry relative to ground: a. two wires above an “infinite” ground plane, and b. two wires symmetric around a ground wire.

characteristic impedance matrix of the type

$$\mathbf{Z}_0 = \begin{pmatrix} R & R_{12} \\ R_{12} & R \end{pmatrix} \quad (28)$$

where R is the characteristic impedance of the single conductor relative to ground (named “single ended mode” in [11]) and R_{12} is the mutual term. The eigenvectors of the characteristic impedance matrix in Eq. (28) are the columns of

$$\mathbf{T} = \begin{pmatrix} -1/\sqrt{2} & 1/\sqrt{2} \\ 1/\sqrt{2} & 1/\sqrt{2} \end{pmatrix}, \quad (29)$$

so that calling the voltages on the physical lines \mathbf{V} , and the modal voltages \mathbf{V}' , we have $\mathbf{V}' = \mathbf{T}^T \mathbf{V}$. Specifically, for $N = 2$, calling the voltages V_1 and V_2 , we obtain the modal voltages

$$V'_{1,2} = (V_2 \mp V_1)/\sqrt{2}, \quad (30)$$

where V'_1 is the differential mode and V'_2 is the common mode. Let us suppose the conductors are close enough so that external noise n_1 and n_2 added to the voltages V_1 and V_2 respectively are closely correlated. This is connected to the rule of maintaining the conductors close to each other [11]. We assume that the statistical averages $\langle n_1 \rangle = \langle n_2 \rangle = 0$, $\langle n_1^2 \rangle = \langle n_2^2 \rangle = \sigma^2$ and $\langle n_1 n_2 \rangle = \rho \sigma^2$, where $\rho \simeq 1$ is the correlation coefficient which is supposed to be close to 1. The modal noises are

$$n'_{1,2} = (n_2 \mp n_1)/\sqrt{2}, \quad (31)$$

so that

$$\langle n'^2_{1,2} \rangle = \sigma^2(1 \mp \rho). \quad (32)$$

For $\rho \simeq 1$, the differential mode noise $\langle n'^2_1 \rangle \simeq 0$ and the common mode noise $\langle n'^2_2 \rangle \simeq 2\sigma^2$. We remark that the sum of the noises power

$$\langle n'^2_1 \rangle + \langle n'^2_2 \rangle = \langle n^2_1 \rangle + \langle n^2_2 \rangle = 2\sigma^2, \quad (33)$$

because the transformation preserves the noise power.

For the general case of MTL, with N conductors and ground, Eq. (33), may be generalized to

$$\sum_{j=1}^N \langle n'^2_j \rangle = \sum_{j=1}^N \langle n^2_j \rangle = N\sigma^2, \quad (34)$$

where we considered again $\langle n^2_j \rangle = \sigma^2$ for any j and it remains to classify the values of $\langle n'^2_j \rangle$. If the condition of an identical geometry of any conductor relative to ground is satisfied, i.e. identical “single ended modes” in [11], the characteristic impedance matrix has identical terms on the diagonal, and only in this case one can still define a “differential mode”, having

a noise power close to 0, like in the example of Figure 3a, representing wires above Printed Circuit Board (PCB) [12]. Following the procedure described in [3, 4], and using the image

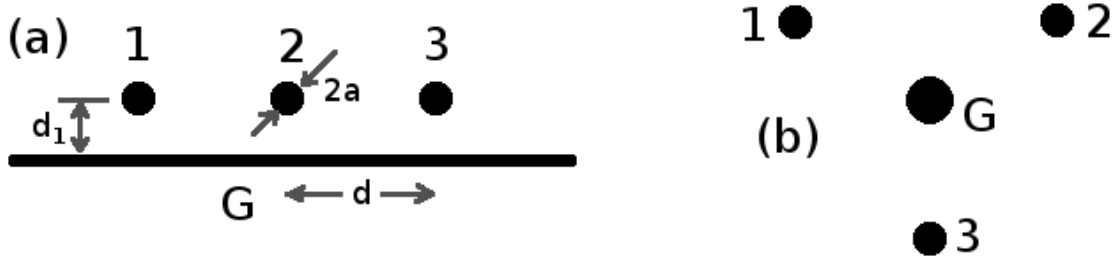


FIG. 3: Cross sections examples of three conductors having the same geometry relative to ground: a. three wires above an “infinite” ground, where we defined the wire radius a , the distance between the wires d and the distance to the ground d_1 , and b. three wires symmetrically arranged around a ground wire.

method, one can calculate analytically the characteristic impedance matrix for $d, d_1 \gg a$, obtaining

$$Z_{0\ ij} = \frac{\eta_0}{2\pi} \begin{cases} \ln \frac{2d_1}{a} & i = j \\ \ln \sqrt{1 + \frac{2d_1}{(j-i)d}} & i \neq j \end{cases}, \quad (35)$$

where $\eta_0 = 377\Omega$ is the free space impedance. For $N = 3$, $d/a = 7.9128$ and $d_1/d = 2$, this results in

$$\mathbf{Z}_0 = \frac{\eta_0}{2\pi} \begin{pmatrix} 3.45477 & 1.41661 & 0.80472 \\ 1.41661 & 3.45477 & 1.41661 \\ 0.80472 & 1.41661 & 3.45477 \end{pmatrix}, \quad (36)$$

having eigenvectors given by the columns of

$$\mathbf{T} = \begin{pmatrix} -0.44808 & -1/\sqrt{2} & 0.54702 \\ 0.77360 & 0 & 0.63368 \\ -0.44808 & 1/\sqrt{2} & 0.54702 \end{pmatrix}. \quad (37)$$

Considering for simplicity the correlations between all pair of noises $\rho = 1$, one gets the modal noises

$$n'_1 = 0.015\sigma^2, \quad n'_2 = 0, \quad n'_3 = 2.985\sigma^2, \quad (38)$$

defining the second mode as the “differential mode”. A very special case of $N = 3$ is shown in Figure 3b, showing identical mutual impedance properties between all pair of conductors.

The characteristic impedance matrix has the form

$$\mathbf{Z}_0 = \begin{pmatrix} R_d & R_{od} & R_{od} \\ R_{od} & R_d & R_{od} \\ R_{od} & R_{od} & R_d \end{pmatrix}, \quad (39)$$

where R_d are the diagonal elements and R_{od} are the off diagonal elements. Such a configuration has two degenerate “differential modes” and one additional mode which may be called in this case the common mode, yielding the following modal noises power (for $\rho = 1$)

$$n'_1 = 0, \quad n'_2 = 0, \quad n'_3 = 3\sigma^2, \quad (40)$$

For the geometry discussed in this paper, shown in Figure 4, each conductor relates differently to the ground, so that there is no “differential” mode and the modal noises come out:

$$n'_1 = 0.013991\sigma^2, \quad n'_2 = 0.061921\sigma^2, \quad n'_3 = 2.9241\sigma^2, \quad (41)$$

To summarize this section: the modes can always be ordered by their noise immunity, from the less noisy mode to the noisiest mode. In case all conductors have the *same geometry* relative to ground, i.e. the characteristic impedance matrix has identical terms on the diagonal, there is always a mode which can be named “differential”, having a very low noise power (0 for very high correlation between the noises developed on the conductors). Degenerate differential modes may also exist when mutual impedances between several pairs of conductors are identical.

As mentioned at the beginning of this section, we used for simplicity lossless examples, but the above conclusions are valid for lossy MTL, provided the above symmetries apply to the losses mechanism too. For example, if the MTL in Figure 2a has copper losses (which are the dominant losses in such configuration due to the thin conductors), the characteristic impedance matrix in Eq. (28) has the form

$$\mathbf{Z}_0 = \begin{pmatrix} R(1 - j\alpha) & R_{12}(1 - j\gamma) \\ R_{12}(1 - j\gamma) & R(1 - j\beta) \end{pmatrix} \quad (42)$$

where α , β and γ are positive (because copper losses result in negative imaginary additions) and usually small, for small losses. The identical values R in Eqs. (28) or (42) on the diagonal are due to the identical geometries of both conductors relative to ground, but this

applies also to the losses, so that $\alpha = \beta$ (unless the conductors are of different materials). The eigenvectors of the characteristic impedance matrix in (42) are still the columns of the matrix in (29) if $\alpha = \beta$, so that the same “differential” and “common” modes arise in the lossy case.

III. ELECTROMAGNETIC SIMULATIONS

We analyze in this section the results of our electromagnetic simulations. We use HFSS commercial ANSYS software (FEM method), to model the MTL into an S parameters block, for all the frequencies we need, and for all the cases we deal with.

Our convergence criterion is as follows: between consecutive iterations, as long as the difference between the absolute values is bigger than 0.005 for each element of the S parameters matrix, the computation continues. This means that the worse converged coefficient of the matrix has an error of 0.005, hence the overall error is much smaller. To learn more on the accuracy of our S parameters matrices we examined how close they are to the structure predicted theoretically in Eq. (1) (i.e. two identical submatrices \mathbf{I} on the diagonal and two identical submatrices $\boldsymbol{\tau}$ on the anti-diagonal) and we found out that our typical error for the S parameters coefficients is around $10^{-4} - 10^{-5}$.

From each S parameters, we calculate a generalized ABCD matrix representation (see Eqs. (5)-(8)) from which we calculate the characteristic impedance eigenvalues of the modes (Eq. (17)), the electrical delay angle of each mode (Eq. (18)) and the pre-processing and post-processing matrices (Eqs. (24)-(25)) needed for a perfect match and for eliminating crosstalk, as explained in section II.

We use the MTL geometry shown in Figure 4, and the cross section in Figure 5 shows the insulator of relative dielectric constant $\epsilon_r = 2.1$, of dimensions 2mm on 6mm (see [1]). We ran four distinct cases: “lossless” (i.e. ideal conductors and $\tan \delta = 0$), “copper losses only” (copper conductors and $\tan \delta = 0$), “dielectric losses only” (ideal conductors and $\tan \delta = 0.001$) and “copper and dielectric losses together” (copper conductors and $\tan \delta = 0.001$). Each case is simulated for the frequencies 50, 100 and 200MHz.

In all the cases, losses being small, the real part of the characteristic impedance matrix eigenvalues, and equivalent relative dielectric constants (or refraction index) of the modes

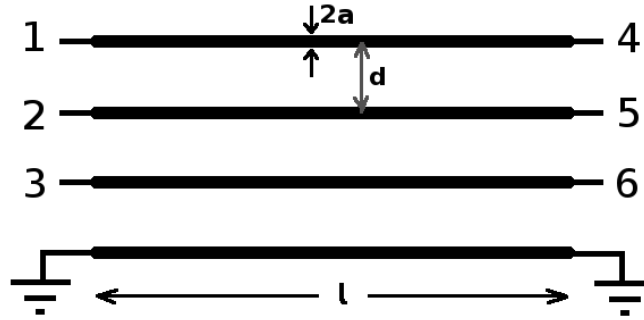


FIG. 4: The geometry is based on flat cables, the conductors are cylindrical with radius $a = 0.1605$ mm, and the distance between their centers is $d = 1.27$ mm. The number of conductors is 4, hence $N = 3$. The MTL length is $l = 20$ cm (the figure is not in proportion due to space limitations). The port number is shown near each terminal, so that the near/far end ports are relative to the near/far end grounds which are of course different electric points, but for simplicity marked with the same ground symbol.



FIG. 5: Cross section of the conductors inside the insulator. The arrows show the electric field for some feeding and one remarks that it is partially in the insulator and partially in the surrounding space. We used the relative dielectric constant $\epsilon_r = 2.1$. We simulated the cases of $\tan \delta$ equal 0 or 0.001 and the cases of copper or ideal conductors.

are essentially like in [1], as follows:

$$Z'_0 = 427.5, 185.5, 88\Omega, \quad (43)$$

$$\epsilon_{eq} = 1.77, 1.99, 2.08 \text{ and } n = \sqrt{\epsilon_{eq}} = 1.33, 1.41, 1.44 \quad (44)$$

and the delay angles are obtained for each mode/frequency by inverting Eq. (19) for θ and using the values in (44).

It is interesting to remark, that if we rescale the eigenvalues of the characteristic impedance matrix by the relative dielectric constants of the modes, and transform back (see Eq. (20))

$$\mathbf{T}_V(\mathbf{Z}'_0\mathbf{n})\mathbf{T}_V^T = \begin{pmatrix} 380.05 & 231.61 & 148.44 \\ 231.61 & 331.4 & 165.7 \\ 148.44 & 165.7 & 248.22 \end{pmatrix} \Omega, \quad (45)$$

we reproduce the free space characteristic impedance matrix, calculated analytically in [3, 4]. This confirms the correctness and accuracy of our simulations.

The imaginary part of the characteristic impedance matrix eigenvalues (Eq. (17)), and of the delay angle (Eq. (18)) resulting from the simulations represent the losses and are given in the following tables for all the modes and all the simulated frequencies. The “lossless” case (for which those imaginary parts should theoretically be 0) are also shown in those tables. In [1] we neglected those imaginary values, considering them numerical simulation errors, but here we will show that they represent radiation losses. For further referencing, we symbolically mark the values for the simulated cases: lossless, copper losses only, dielectric losses only and copper and dielectric losses by x , y , z and w , respectively.

The following tables I-III show the simulation results for the imaginary parts of the characteristic impedance matrix eigenvalues $\text{Im}\{Z'_0\}$, and the delay angles $\text{Im}\{\theta\}$, for the frequencies 50, 100 and 200MHz, respectively. One remarks that $\text{Im}\{Z'_0\}$ is negative in the case of copper losses only and positive in the case of dielectric losses, as happens in the case of a two-conductor transmission line (TL). For the lossless case (which actually shows radiation losses) $\text{Im}\{Z'_0\}$ may be either positive or negative. It comes out that for the case of copper and dielectric losses, $\text{Im}\{Z'_0\}$ is negative, showing that copper losses are dominant. The values for $\text{Im}\{\theta\}$ are negative in all cases, representing an exponential decay of the forward moving waves.

TABLE I: Imaginary parts of the characteristic impedance eigenvalues Z'_0 in units of Ω and of the electric delay angle of the modes θ for frequency 50MHz

| | Lossless (x) | Copper only (y) | Dielectric only (z) | Copper and Dielectric (w) | |
|-----------------|------------------|---------------------|-------------------------|-------------------------------|-------------|
| Im $\{Z'_0\}$ | mode 1 | -0.028904 | -1.529 | 0.11297 | -1.3887 |
| | mode 2 | 0.2343 | -1.0609 | 0.34403 | -0.97514 |
| | mode 3 | 0.15709 | -0.91779 | 0.19479 | -0.87316 |
| Im $\{\theta\}$ | mode 1 | -1.5105e-04 | -1.4782e-03 | -2.5111e-04 | -1.5782e-03 |
| | mode 2 | -7.6636e-06 | -2.1563e-03 | -1.4449e-04 | -2.2938e-03 |
| | mode 3 | -7.316e-06 | -2.658e-03 | -1.5576e-04 | -2.8075e-03 |

TABLE II: Imaginary parts of the characteristic impedance eigenvalues Z'_0 in units of Ω and of the electric delay angle of the modes θ for frequency 100MHz

| | Lossless (x) | Copper only (y) | Dielectric only (z) | Copper and Dielectric (w) | |
|-----------------|------------------|---------------------|-------------------------|-------------------------------|-------------|
| Im $\{Z'_0\}$ | mode 1 | 0.032535 | -1.0106 | 0.1683 | -0.8632 |
| | mode 2 | 0.32629 | -0.62117 | 0.45631 | -0.55127 |
| | mode 3 | 0.23026 | -0.53842 | 0.34604 | -0.4724 |
| Im $\{\theta\}$ | mode 1 | -6.2666e-04 | -2.4919e-03 | -8.2367e-04 | -2.6939e-03 |
| | mode 2 | -2.0782e-05 | -3.0513e-03 | -2.891e-04 | -3.3239e-03 |
| | mode 3 | -9.6385e-06 | -3.7457e-03 | -3.0351e-04 | -4.0415e-03 |

TABLE III: Imaginary parts of the characteristic impedance eigenvalues Z'_0 in units of Ω and of the electric delay angle of the modes θ for frequency 200MHz

| | Lossless (x) | Copper only (y) | Dielectric only (z) | Copper and Dielectric (w) | |
|-----------------|------------------|---------------------|-------------------------|-------------------------------|-------------|
| Im $\{Z'_0\}$ | mode 1 | 0.042204 | -0.68227 | 0.18483 | -0.54387 |
| | mode 2 | 0.17168 | -0.52052 | 0.2617 | -0.4359 |
| | mode 3 | -0.015032 | -0.59712 | 0.036131 | -0.5478 |
| Im $\{\theta\}$ | mode 1 | -2.4341e-04 | -5.0905e-03 | -2.8327e-03 | -5.4899e-03 |
| | mode 2 | -6.2179e-05 | -4.3822e-03 | -6.0848e-04 | -4.9297e-03 |
| | mode 3 | -3.2523e-05 | -5.343e-03 | -6.2514e-04 | -5.9409e-03 |

IV. CONSISTENCY OF THE SIMULATION RESULTS

In principle one expects the simulation results for copper and dielectric losses to reproduce the sum of the losses of the individual separate simulations (for copper losses and dielectric losses), i.e. the simulation results for copper and dielectric losses should reproduce the sum for the imaginary values (for Z'_0 or θ) from the individual simulations. One may check that this does not come out, and the explanation for this is the presence of radiation losses in all the simulations.

If indeed the simulations detected radiation losses (which are the only losses in the case we called “lossless”), it means that the values marked symbolically with x , represent radiation losses. Those being present also in the “copper only” simulations, for which the imaginary results have been marked symbolically with y , it means that y includes radiation and copper losses.

By the same logic, the “dielectric only” simulations, for which the imaginary results have been marked symbolically with z , contain *radiation and dielectric* losses, and the “copper and dielectric” simulations, for which the imaginary results have been marked symbolically with w , contain *all* the losses, i.e. radiation, copper and dielectric.

Hence, to obtain the true copper losses effect one has to compensate the radiation losses, so that they are obtained from $y - x$, and so the true dielectric losses effect are obtained from $z - x$ and the total copper and dielectric losses effect is obtained from $w - x$. Therefore, to check the consistency of the simulation results, one has to check that $(y - x) + (z - x) = (w - x)$, or $w = y + z - x$.

In table IV we compare the simulation results for the case of copper and dielectric losses, marked by w (and actually representing all the losses), with the simulation results from the “copper only” case (y) plus with the simulation results from the “dielectric only” case (z), minus the simulation results from the “lossless” case (x , which actually contains the radiation losses only). The results in table IV confirm that our assumption of the detection of radiation losses in all the simulations is correct, and the values compare very well, showing an average deviation of 1.5% between the results. The maximum deviation is of 10%, but we notice that those imaginary parts of Z'_0 are small fractions of the real part of Z'_0 in Eq. (43), so that larger deviations for small values is possible.

TABLE IV: Comparison between the imaginary values obtained by the simulation with copper and dielectric losses, called w and the combination of the imaginary values obtained by the separate simulations, called $y + z - x$. The table on the left side compares the imaginary part of Z'_0 (in units of $[\Omega]$), and the table on the right side compares the imaginary part of θ .

| Frequency | w | $y + z - x$ | Frequency | w | $y + z - x$ |
|-----------|--------|-------------|-----------|-------------|-------------|
| 50MHz | mode 1 | -1.3887 | mode 1 | -1.5782e-03 | -1.5783e-03 |
| | mode 2 | -0.97514 | mode 2 | -2.2938e-03 | -2.2931e-03 |
| | mode 3 | -0.87316 | mode 3 | -2.8075e-03 | -2.8064e-03 |
| 100MHz | mode 1 | -0.8632 | mode 1 | -2.6939e-03 | -2.6891e-03 |
| | mode 2 | -0.5513 | mode 2 | -3.3239e-03 | -3.3404e-03 |
| | mode 3 | -0.4724 | mode 3 | -4.0415e-03 | -4.04e-03 |
| 200MHz | mode 1 | -0.54387 | mode 1 | -5.4899e-03 | -5.4892e-03 |
| | mode 2 | -0.4359 | mode 2 | -4.9297e-03 | -4.9285e-03 |
| | mode 3 | -0.5478 | mode 3 | -5.9409e-03 | -5.9356e-03 |

V. COMPARISONS WITH TWIN LEAD TWO-CONDUCTOR TL

A two conductor transmission line (TL) propagates one single propagation mode, while for a MTL of N conductors and ground, one has N propagation modes, in our example from Figure 4, $N = 3$. So when comparing properties of a MTL mode with the single mode of a two conductors TL, one may expect some similarities if these properties are governed by same physical processes. The most resembling two-conductor TL to the MTL analyzed in this work is the twin lead TL, hence we shall compare some results with it.

The characteristic impedance for a lossy two-conductor TL may be written as

$$Z_0 = \sqrt{\frac{R + j\omega L}{G + j\omega C}} \simeq Z_{00} + j(Z_{0\text{copper}} + Z_{0\text{dielectric}}) \quad (46)$$

where L , C , R and G are the per length unit inductance, capacitance, serial resistance and parallel conductance and $Z_{00} = \sqrt{L/C}$ is the real part of Z_0 , and also its main part, given small losses, and

$$Z_{0\text{copper}} = -\frac{Rc}{2\omega\sqrt{\epsilon_{eq}}} \quad (47)$$

$$Z_{0\text{dielectric}} = \frac{Z_{00} \tan \delta_{eq}}{2} \quad (48)$$

are the imaginary parts of Z_0 due to copper and dielectric losses, respectively. In Eq. (47) c is the speed of light in vacuum, ϵ_{eq} is the equivalent relative dielectric constant and $\omega = 2\pi f$ is the angular frequency. In Eq. (48) $\tan \delta_{eq}$ is the equivalent loss tangent, taking into account the part of the fields in air.

The value of Z_{00} is not directly related to the characteristic impedance eigenvalues Z'_0 . For example for a twin lead with the parameters from Figure 4 in free space, $Z_{00} = 246.26\Omega$, while an MTL as in Figure 4 in free space has the characteristic impedance eigenvalues: 108.06, 153.91 and 697.69 Ω [3, 4], which is easily verified by diagonalizing Eq. (45). However, $Z_{0\text{copper}}$ in Eq. (47) does not depend on Z_{00} , but rather on the per length unit resistance R , which for a twin lead is:

$$R = \frac{2}{\sigma \delta p}, \quad (49)$$

where the factor 2 is due to two conductors, $\sigma = 5.8e7$ S/m is the copper specific conductance, $\delta = \sqrt{\frac{2}{\omega \mu_0 \sigma}}$ is the skin depth and $p = 2\pi a = 1\text{mm}$ is the perimeter (or circumference) of the conductors (see Figure (4)). In table V we compare the imaginary part of the characteristic impedance eigenvalues obtained from the simulation due to copper losses only, with

TABLE V: Comparison between the $\text{Im}\{Z'_0\}$ (in units of $[\Omega]$) due to copper losses only, obtained by the simulation vs. Eq. (47). The copper losses effect is obtained by compensating for the radiation losses, i.e. by using the results for “copper only” minus the results for “lossless”, which we mark by $y - x$.

| Frequency | $y - x$ | Analytic | |
|-----------|---------|----------|----------|
| 50MHz | mode 1 | -1.5001 | -1.3125 |
| | mode 2 | -1.2952 | -1.2367 |
| | mode 3 | -1.0749 | -1.2096 |
| 100MHz | mode 1 | -1.04313 | -0.92903 |
| | mode 2 | -0.94746 | -0.8755 |
| | mode 3 | -0.76868 | -0.85636 |
| 200MHz | mode 1 | -0.72447 | -0.6571 |
| | mode 2 | -0.6922 | -0.61907 |
| | mode 3 | -0.58209 | -0.60555 |

Eq. (47). In Eq. (47) we use the ϵ_{eq} for the modes given in Eq. (44) and as explained before,

the copper losses effect is obtained from the simulation after compensating for the radiation losses, i.e. by using the values marked by $y - x$. The average of the absolute error is 9.2%.

The electric delay angle for a lossy two-conductor TL may be written as

$$\theta = \omega l \sqrt{[L + R/(j\omega)][C + C/(j\omega)]} \simeq \theta_0 + j(\theta_{copper} + \theta_{dielectric}) \quad (50)$$

where $\theta_0 = \omega l \sqrt{LC}$ is the real part of θ , and also its main part, given small losses, and

$$\theta_{copper} = -\frac{\sqrt{\epsilon_{eq}} R l}{2\eta_0} \quad (51)$$

$$\theta_{dielectric} = -\frac{\theta_0 \tan \delta_{eq}}{2} \quad (52)$$

are the imaginary parts of θ due to copper and dielectric losses, respectively. Eq. (52) can be inverted to

$$\frac{\tan \delta_{eq}}{\tan \delta} = -\frac{2\theta_{dielectric}}{\theta_0 \tan \delta}, \quad (53)$$

and this is expected to be almost frequency independent, because we used a relative dielectric

TABLE VI: Comparison between results of $\tan \delta_{eq}/\tan \delta$ obtained from the simulation (Eq. (53)) vs. those obtained from the analytic equation (54). The simulation results are elaborated from the results obtained for “dielectric losses only” (marked by z) minus the results obtained from the “lossless” simulation (marked by x), and the results are almost frequency independent. For the analytic formula we used ϵ_{eq} from Eq. (44).

| Mode | Simulation result | Analytic result |
|------|-------------------|-----------------|
| 1 | 0.72 | 0.82 |
| 2 | 0.92 | 0.95 |
| 3 | 0.98 | 0.99 |

constant which is frequency independent. This may be compared with the ratio given in [9] and defined there as a “filling factor”:

$$\frac{\tan \delta_{eq}}{\tan \delta} = \frac{\epsilon_r(\epsilon_{eq} - 1)}{\epsilon_{eq}(\epsilon_r - 1)}, \quad (54)$$

which compensates for the part of the fields in air, so that if $\epsilon_{eq} = \epsilon_r$ (all the fields are inside the dielectric), $\tan \delta_{eq} = \tan \delta$ and if $\epsilon_{eq} = 1$ (all the fields are in the air), $\tan \delta_{eq} = 0$. In table VI we compare the values for $\tan \delta_{eq}/\tan \delta$ obtained from simulation (Eq. (53)) vs. the values obtained from Eq. (54). The average absolute error of this comparison is 6%.

VI. THE CROSSTALK ELIMINATION ALGORITHM ON THE LOSSY MTL

We tested the crosstalk elimination algorithm on the MTL with copper and dielectric losses, using the circuit described in Figure 6 for the simulations. The post and pre-

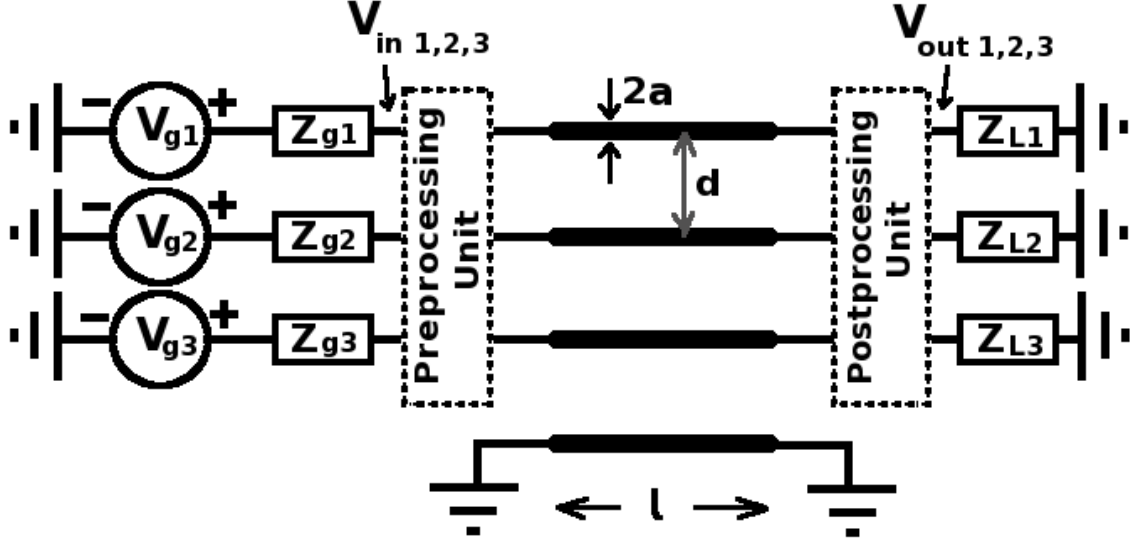


FIG. 6: The geometry and the physical dimensions ($a = 0.1605$ mm, $d = 1.27$ mm and $l = 20$ cm) are described in Figure 4, and shown again here, for convenience. The conductors 1, 2 and 3 are fed by $V_{g_i} = 2V$ with an internal impedance of $Z_{g_i} = 50\Omega$, at 50, 100 and 200MHz respectively (which represent forward voltages of 1V through transmission lines of 50Ω), and are loaded at the far end with $Z_{L_i} = 50\Omega$. The conductors are numbered up-down by 1, 2 and 3 and the grounded conductor is the common.

processing units are designed according to Eqs. (24) and (25), but in our case of losses the transformation \mathbf{T}_V is complex and frequency dependent and so are the processing units \mathbf{G}_{pre} and \mathbf{G}_{post} .

However, as explained in section II, the transformation matrices \mathbf{T}_V and \mathbf{T}_I are approximately real and frequency independent, and their imaginary and/or frequency dependent parts are due to losses, and so are the processing units, according to Eqs. (24) and (25).

Now mathematically we can implement any complex frequency dependent processing unit, but thinking of a future implementation, it would be much simpler and more advantageous to implement real transformations. Such an implementation should be robust and

for all frequencies, anticipating the system to run signals in a certain frequency range. Certainly, those transformations do not diagonalize exactly, hence we expect a degradation in performance.

For this reason we chose to use the real part of \mathbf{T}_V to calculate the necessary processing units \mathbf{G}_{pre} and \mathbf{G}_{post} . Given the fact we used frequencies 50, 100 and 200MHz, we chose to use \mathbf{T}_V for a middle frequency in the range, i.e. 100MHz. We obtain:

$$\mathbf{G}_{pre} = \begin{pmatrix} 2.3265 & 0.003883 & 0.57064 \\ 1.643 & 1.3676 & -0.51352 \\ 0.67822 & 1.3633 & 1.0902 \end{pmatrix}. \quad (55)$$

and $\mathbf{G}_{post} = \mathbf{G}_{pre}^{-1}$, because we used load impedances equal to generator impedances (see Eqs. (24) and (25)).

In table VII we present the results obtained from the ‘‘Designer’’ software which uses the S matrices obtained from the electromagnetic simulations with copper and dielectric losses, representing the MTL in the circuit described in Figure 6 (implemented once with the processing units, and once without them). For the case of using the processing units,

TABLE VII: Voltages V_{in} and V_{out} measured by Designer for the circuit described in Figure 6. Magnitude is in [V], phase is in degrees and the upper row shows the frequencies in [MHz].

| | With processing units | | | No processing units | | |
|------------|--------------------------|--------------------------|-------------------------------|------------------------------|-----------------------------|-----------------------------|
| f | 50 | 100 | 200 | 50 | 100 | 200 |
| V_{in1} | 1 ∠- 0.096 | 0.448m∠-110.31 | 0.377m∠-131.22 | 1.375 ∠ 12.83 | 0.29∠4.04 | 0.076∠-36.63 |
| V_{in2} | 0.227m∠-98.547 | 1 ∠ 0 | 0.926m∠-145.36 | 0.28 ∠25.77 | 1.44 ∠ 8.68 | 0.202∠-0.48 |
| V_{in3} | 0.372m∠-94.4 | 0.55m∠-117.35 | 1 ∠- 0.225 | 0.167∠14.81 | 0.226 ∠10.15 | 1.604 ∠ 4.98 |
| V_{out1} | 1 ∠- 16.05 | 0.023m∠-73.694 | 0.396m∠101.74 | 0.765 ∠- 31.58 | 0.28∠158.12 | 0.137∠ 112.19 |
| V_{out2} | 0.0141m∠29.856 | 1 ∠- 34.04 | 0.0758m∠-133.99 | 0.252∠-166.67 | 0.71 ∠- 43.01 | 0.212∠ 113.92 |
| V_{out3} | 0.103m∠-153.88 | 0.018m∠-20.15 | 0.994 ∠- 69.546 | 0.163∠-170.91 | 0.21∠161 | 0.71 ∠- 72.95 |

ideally in case of complete crosstalk elimination and perfect match, the input voltages $V_{in1,2,3}$ on the diagonal (written with bold face) should have been 1∠0, according to Eq. (26). We see that the 100MHz behaves best, probably because we used the \mathbf{T}_V transformation obtained for 100MHz to compute the processing units. Also, in the ideal case, the output voltages

$V_{out1,2,3}$ on the diagonal (written with bold face) should have been $1\angle\theta_{1,2,3}$, where $\theta_{1,2,3}$ are the delay angles of 50MHz on mode 1, 100MHz on mode 2 and 200MHz on mode 3, respectively, according to Eq. (27). The theoretical values for those angles is 15.951° , 33.862° and 69.235° , respectively. All the small non bold values in table VII, should have been ideally 0, and they are 3 order of magnitude smaller than 1V, when using the processing units.

Without processing units, we see the crosstalk also at the input, i.e. in the $V_{in1,2,3}$ voltages and also at the output voltages $V_{out1,2,3}$. Still the excited frequency at the given port, has a higher value than the others, and has been marked by bold face. For example the 50MHz has been applied at port 1, and we see that for 50MHz, $V_{in1} = 1.375V$, while the crosstalk values $V_{in2,3}$ are 0.28V and 0.167V, respectively and are smaller than V_{in1} .

The results shown in table VII are plotted in time in Figure 7. In the left group of plots,

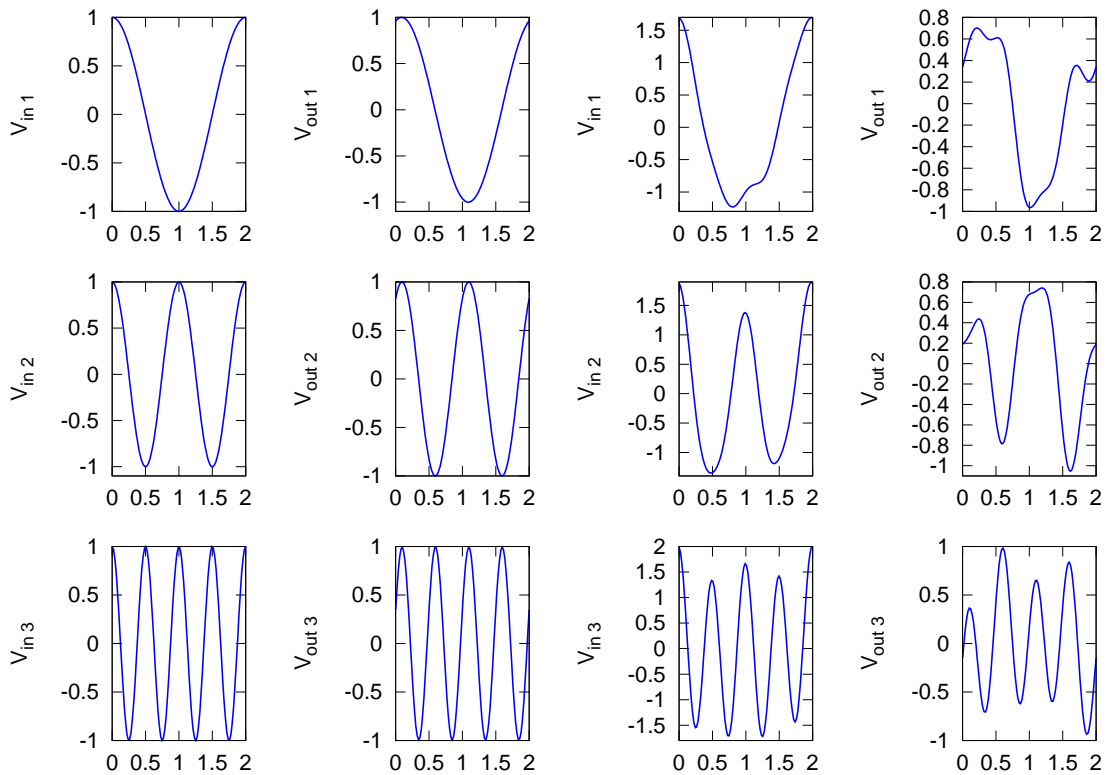


FIG. 7: Plots of the input and output voltages in time. The left group of plots shows the input and output voltages for the case the processing units are active, and the right group of plots shows the same voltages without the processing units. All the horizontal axes are in units of 10^{-8} sec, so that this time range fits to one cycle of 50MHz.

which has been obtained with active processing units, we see almost clean harmonics of

50, 100 and 200MHz at ports 1, 2 and 3 respectively (negligible crosstalk), and the output voltages have the same amplitudes as the input voltages, shifted by the adequate phase, emphasizing a very good impedance match. In the right group of plots, obtained without the processing units, we distinguish a “main” frequency of 50, 100 and 200MHz at ports 1, 2 and 3 respectively, but each signal is mixed with the other frequencies, due to crosstalk.

VII. CONCLUSIONS

We analyzed in this work the properties of lossy MTL in an open (flat cables like) geometry. We checked separately and together, copper and dielectric losses, and we showed that the simulations detected radiation losses in all the simulated cases.

We also obtained a good comparison between the losses characteristics of individual MTL modes with two conductor TL, in cases in which this is physically justified.

We applied the crosstalk elimination algorithm developed in [1] to MTL with copper and dielectric losses. Because losses are frequency dependent, the idea is to design the algorithm for a “middle frequency” in the relevant frequency range (in our case 100MHz) and use it for all frequencies. The algorithm works well and gradually degrades with the increase in losses.

As mentioned in the introduction, this algorithm has the potential to increase the information rate, but this gain is also subject to the noise immunity of the modes (analyzed in this work), so that less gain is possible in noisy environments, according to Shannon’s law. This issue is open for further research.

-
- [1] Vulfin V. and Ianconescu R., “Transmission of the maximum number of signals through a Multi-Conductor transmission line without crosstalk or return loss: theory and simulation”, *IET MICROW ANTENNA P*, 9(13), pp. 1444-1452 (2015)
 - [2] Ianconescu R. and Vulfin V., “Simulation of lossy multiconductor transmission lines and application of an algorithm to reduce crosstalk”, 2015 IEEE International Conference on Microwaves, Communications, Antennas and Electronic Systems (COMCAS), Tel-Aviv, 2-4 Nov, 2015

- [3] Ianconescu R., "TEM waves guided between many conductors", *Modern Applied Science*, 2013, 7,(12), pp. 90-107
- [4] Ianconescu R. and Vulfin V., "Simulation for a Crosstalk Avoiding Algorithm in Multi-Conductor Communication", 2014 IEEE 28-th Convention of Electrical and Electronics Engineers in Israel, Eilat, December 3-5, 2014
- [5] Ianconescu R., "Polyphase guided TEM waves", *2012 IEEE 27-th Convention of Electrical and Electronics Engineers in Israel*, Eilat, November 14-17, 2012
- [6] Ianconescu R., "Avoiding crosstalk in multiconductor TEM waveguides", *2013 IEEE International Conference on Microwaves, Communications, Antennas and Electronic Systems*, Tel-Aviv, 21 Oct - 23 Oct, 2013
- [7] Paul C. R., "Analysis of Multiconductor Transmission Lines", (New York: Wiley, 2nd edition 2008).
- [8] Staelin D. H., Morgenthaler A., Kong J. A., "Electromagnetic Waves", (Prentice Hall, 1994)
- [9] Pozar D. M., "Microwave Engineering", (Wiley India Pvt., 2009)
- [10] Orfanidis S.J., "Electromagnetic Waves and Antennas", ISBN: 0130938556, (Rutgers University, 2002)
- [11] Brooks D., "Differential Signals Rules to live by", *Printed Circuit Design*, (a CMP Media publication, 2001)
- [12] Brooks D., "PCB Currents: How They Flow, How They React" (Prentice Hall Modern Semiconductor Design), 1st Edition (2013)